Comparison of global and local damage in reinforced concrete columns specimens

R. Kliukas*, R. Kačianauskas**

*Vilnius, Gediminas Technical University, Saulėtekio al. 11, LT-10223 Vilnius-40, Lithuania, E-mail: pirmininkas@adm.vtu.lt
**Vilnius, Gediminas Technical University, Saulėtekio al. 11, LT-10223 Vilnius-40, Lithuania, E-mail: rkac@fm.vtu.lt

1. Introduction

Many columns, piers and towers used in nuclear engineering, civil engineering, road construction, power engineering, offshore engineering and several other fields, are made of high-strength structural concrete. High-strength concrete differs from the usual concrete in compressive strength ($f_c = 50$-150 MPa), tensile resistance ($f_t = 5$-15 MPa), durability, and also on the resistance to abrasion, aggressive environment and temperature gradient. The potential applications are almost countless. During the last two decades the research developed rapidly and the use in construction expanded greatly. A comprehensive reviews on the matter of subject related to technology development and potencial areas of application may be found in [1-4]. Research on high-strength concrete in Lithuania started in the nineties [5].

In spite of the existence of numerical methods and design codes for evaluating the behavior of high-strength concrete structures, experimental testing still remains the most powerful and reliable research tool. Advanced and innovative experimental techniques, using computer-controlled displacements, provide the base for a realistic simulation. The tests of structural members submitted to a simultaneous combination of longitudinal and transverse loading belong to the category of the most complicated experiments to perform.

For that purpose two main experimental techniques are used, namely, reaction wall/floor systems and shaking tables. It should be noted that computer controlled imposed displacements may be considered as a common feature for both techniques. In the reaction wall/floor systems, in spite of sometimes very complicated dynamic loading history, the external loading may be considered as quasi-static, since the corresponding velocities are very small, consequently only the mechanical properties that are invariable in respect to the velocities can be correctly analyzed. This technique allows full-scale specimens to be tested but not under true inertial forces and real time.

Shaking table testing, started its development in the early fifties and remains an essential tool in earthquake engineering research. Using of it allows the study of true inertial forces acting on the specimens. However, the models are normally constructed at reduced scale, which can limit the scope of the tests.

Several shaking tables throughout the European Union [6], as well as in USA [7] and Japan [8], are being used to perform research about the dynamic effects on civil engineering structures. For that purpose a specific type of triaxial shaking table was designed and built in the Portuguese National Laboratory for Civil Engineering (LNEC) in Lisbon [9-10], consisting of a large rectangular platform (or table), where the test specimens are fixed and shaken, having the three translations controlled and the three rotations mechanically inhibited.

The experimental investigation, presented here, was performed on reinforced high-strength concrete column under horizontal and vertical loading. Two identical column specimens with annular cross-section and spiral reinforcement were designed and two tests, up to failure, were carried out at the LNEC shaking table facility. Accumulation of the global damage of the entire specimen and the local damage at the specified region near the column footing was investigated. The damage concept used here is based on stiffness degradation. Damage accumulation is illustrated by the experimental results.
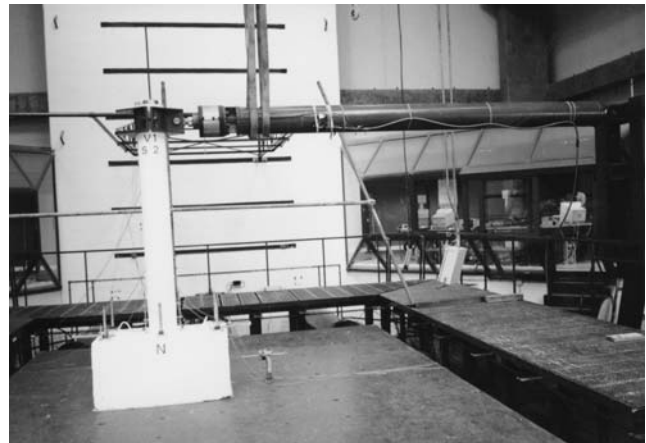
Fig. 1 The view of specimen on shaking table

2. Description of experiment and basic data

Two identical reinforced concrete specimens V1 and V2 with annular cross-section and spiral containment were designed and twice tested up to failure. The entire specimens were produced as monolithic units consisting of a massive footing and a specified column. The view of the specimen on the shaking table is presented in Fig. 1. They have been erected using high-strength concrete with about $f_c = 80$ MPa. Those columns have a wall thickness of 60 mm. Longitudinal reinforcement consisted of 8 bars of 10 mm diameter and transverse reinforcement was a spiral made up with 6 mm diameter bars spaced 50 mm at the critical section. The mechanical properties of the concrete used for the columns as well as for the lower strength footing were evaluated by standard compression tests, performed by a series of cubic and cylindrical probes.
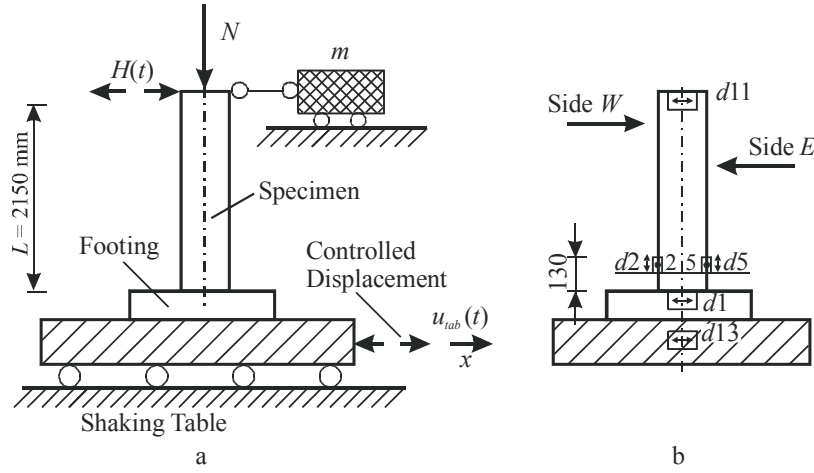
Fig. 2 Illustration of experiment: a - geometry of the specimen and forces, b - location of the displacement transducers

The tested columns were considered as vertical cantilever beams loaded by combined vertical and horizontal actions (Fig. 2, a). A vertical load of $N = 187.5$ kN, producing the axial force, was applied before the tests and remained constant during the entire testing period. It was implemented by prestressing a cable positioned inside the column, at its centre line, and connected from the top of the column to a hollow zone under the footing.

The horizontal time-dependent loading was produced by the motion of the shaking table and by inertia mass involving a set of external additional masses and a connecting rod. The total value of this mass was $m = 12$ t. The motion of the shaking table was prescribed as a function of the transverse horizontal time-dependent displacement.

The sine type loading signals for each of six stages denoted as $S1$ until $S6$ consisted specifically of one initial sine sweep, four successive sine wave stage of increasing amplitude and a final longer sine sweep.

Optical and inductive transducers were used to measure the displacements at preselected points of the specimens. The positions of these displacement transducers, measuring the transverse displacements used in the current presentation, are shown in Fig. 2, b. Transducer $d11$ was used to measure the transverse (in plane) displacement of the column top, while transducer $d13$ has measured the imposed transverse displacements of the shaking table itself. Any eventual sliding of the footings on the shaking table was measured by the inductive transducer $d1$. Data obtained by these measurements was used to investigate the global damage.

In order to monitor local damage, vertical (longitudinal) displacements of the point 2, located on the W side, and the point 5, located on the E side, were registered. The local processing zones on the W side and the E side, are characterized by the respective length $L = 130$ mm. Vertical displacements with respect to the column footing were measured by the inductive displacement transducers $d2$ and $d5$.

Horizontal force $H(t)$, generated at the top of the column, was measured by a loading cell, inserted as part of the connecting rod between the specimens and the inertial mass. Details on general testing procedure may be found in [11-12], while details about the investigation of local damage in [13-14].

3. Damage model

The concept of damage was probably first introduced by Kachanov [15]. Nowadays, even the definition of the damage variables is non-unique. Damage, generally speaking, can be interpreted as a decay of mechanical properties with increasing stress and/or strain.

Continuum damage mechanics (CDM) deals with irreversible processes of elastic continuum with may be also coupled with plasticity, for example [16]. This approach is applicable to different materials including the high strength concrete. The HSC possess, however, anisotropic elastic-brittle damage behaviour while several models aimed to modify the constitutive equations and the damage evolution laws appeared to describe the accumulation of damage for different loadings in the framework of CDM [17]. Continuum damage mechanics presents a local approach assuming that it is possible to establish a damage evolution law for a damage parameter at each point of the structure. Such approach can not be easily extrapolated to entire structure. To avoid the above difficulties, a global approach considering the entire structure damage may be used. In this case, damage evolution is related not only to the material properties but also to the geometry, the construction of the entire structure, loading history, etc. Discussion on these global/local damage concepts may be found in [18]. Damage model, indecently local or global, may be described in the following way.

Non-linear time-dependent behavior of damage zone (local processing zone or entire structure) may be described in terms of horizontal top displacement $u(t)$ and horizontal force $H(t)$

$$K(t)u(t) = H(t) \tag{1}$$

where K is stiffness. Using the definition of continuum damage mechanics $K(t)$ may be considered as the effective stiffness, which decreasing results basically from the increasing of the damage index $d(t)$

$$K(t) = K_0(1 - d(t)) \tag{2}$$

The scalar variable $d(t)$ ($0 \le d(t) \le 1$) represents the reduction on the stiffness $K(t)$, $(K_0 \ge K(t) \ge K_{min})$

compared to its virgin value K_0. A damage index may then be expressed in a traditional way

$$d(t) = \frac{K_0 - K(t)}{K_0 - K_{min}} \qquad (3)$$

Progressive reduction of stiffness is a fact, as it was experimentally observed in the structure behaviour. The stiffness value may be defined as the tangent of the loading curve and obtained considering the horizontal load $H(t)$ and displacement $u(t)$

$$K(t) = |H(t)/u(t)| \qquad (4)$$

The above damage model (1)-(4) was applied to investigate the accumulation of global and local damage as well.

4. Results and discussion

Global behaviour of the column during cyclic loading may be described by a force-displacement curve $H - u$. Here u means relative displacement u_G of the top point with respect to the bottom of column, thus $u \equiv u_G$. Here displacement u actually means strain e_{ij} of the external layer of local processing zone between points i and j, thus $u \equiv e_{ij}$. The time-dependent horizontal force $H(t)$ was measured directly during the experiment, while the horizontal time-dependent displacement $u_G(t)$ was obtained indirectly. It may be expressed as the difference between the displacements at the top and the bottom. The absolute top displacement is directly recorded by transducer d11. The bottom displacement, actually, is the controlled displacement of the shaking table, which is recorded by d13, corrected by the relative displacement of the specimen base in respect with shaking table which is recorded by d1.

Local behaviour of the column near the footing may be described in the same manner using curve $H - u$. It is recorded independently on both sides by transducers d2 and d5.

Character and basic features of the force displacement curves are illustrated on the specimen V2 behaviour at stages S2 and S4 (Fig. 3). Strains e02 and e24 exhibit local behaviour between bottom and point 2 as well as between point 2 and 4. The values of these curves are used for the evaluation of the effective stiffness according to (4).

Normalization of the scale for damage accumulation is rather sophisticated task because exact evaluation of the stiffness limits K_0 and K_{min} is based on heuristic considerations. Virgin value of the stiffness K_0 corresponds to elastic stiffness at the first loading stage S1, while stiffness value at the end of stage S5 is used as minimal stiffness value K_{min}. Finally, time variation of the global damage index $d(t)$ is obtained according to (3).

The picture of the entire damage evolution during stages ranging from S1 to S2 in the specimens V1 and V2 is presented in Fig. 4 and Fig. 5, respectively. Each graph exposes three curves – global damage curve as well as two

curves of the local damage representing local damages on both sides E and W of the specimen.

To compare global and local behaviour of the specimens we propose two independent global damage parameters, as it obvious by the description of damage in the concrete, for example [19]. The first parameter corresponds to bending with compression of the side W while the second one – compression of the side E, respectively.

Both parameters in the case of global damage may be selected from the single global force-displacement curve.

Damage index in one half of the loading cycle reflects compression of one side, while the same index in the second half reflects compression the opposite side. In the case of local damage both parameters are directly computed from two different local force-displacement curves corresponding to two different sides.

Resulting damage of specimens is characterized by envelope curves. Envelopes of the global damage and the local damage are presented for specimen V1 are presented in Fig. 6, a, while envelopes for specimen V2 are presented in Fig. 6, b.
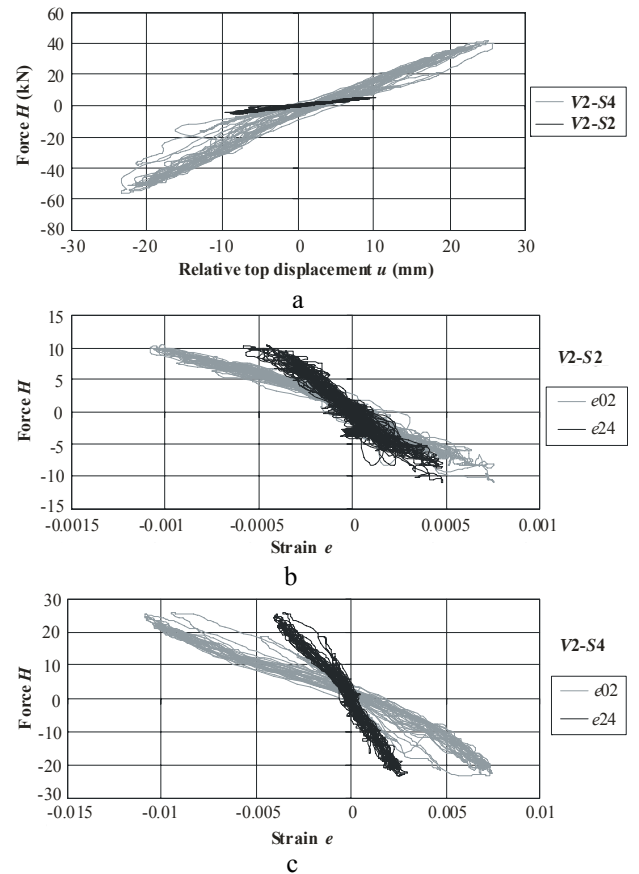
Fig. 3 Force-displacement curves on the specimen V2 at stages S2 and S4: a - global behaviour $H - u_G$; b, c - local behavior $H - e_{ij}$

The graphs illustrate the damage change within separate loading stage. Detailed calculation procedure is illustrated in Table 1 and Table 2. Experimental peak values of force and displacement and corresponding stiffness and global damage index for various time intervals are presented in Table 1, while experimental peak values of force and displacement and corresponding stiffness and local damage index are presented in Table 2.

On the basis of these values and experimental observations, the evolution of global damage conditionally may be divided into three phases – microcracking phase, macrocracking phase and failure phase. The first phase is limited by the development of microcracks, where tension stresses in concrete are beyond the tension resistance. This phase corresponds to loading stages $S1$ and $S2$. During the stage $S1$ the specimen was subjected by low values of horizontal force and behaviour of it was purely elastic with no evidence of macrocracking. At the stage $S2$ three small macrocracks on both sides have been observed. The above mentioned first cracks were closed and hardly observed after unloading due to compression of longitudinal load.
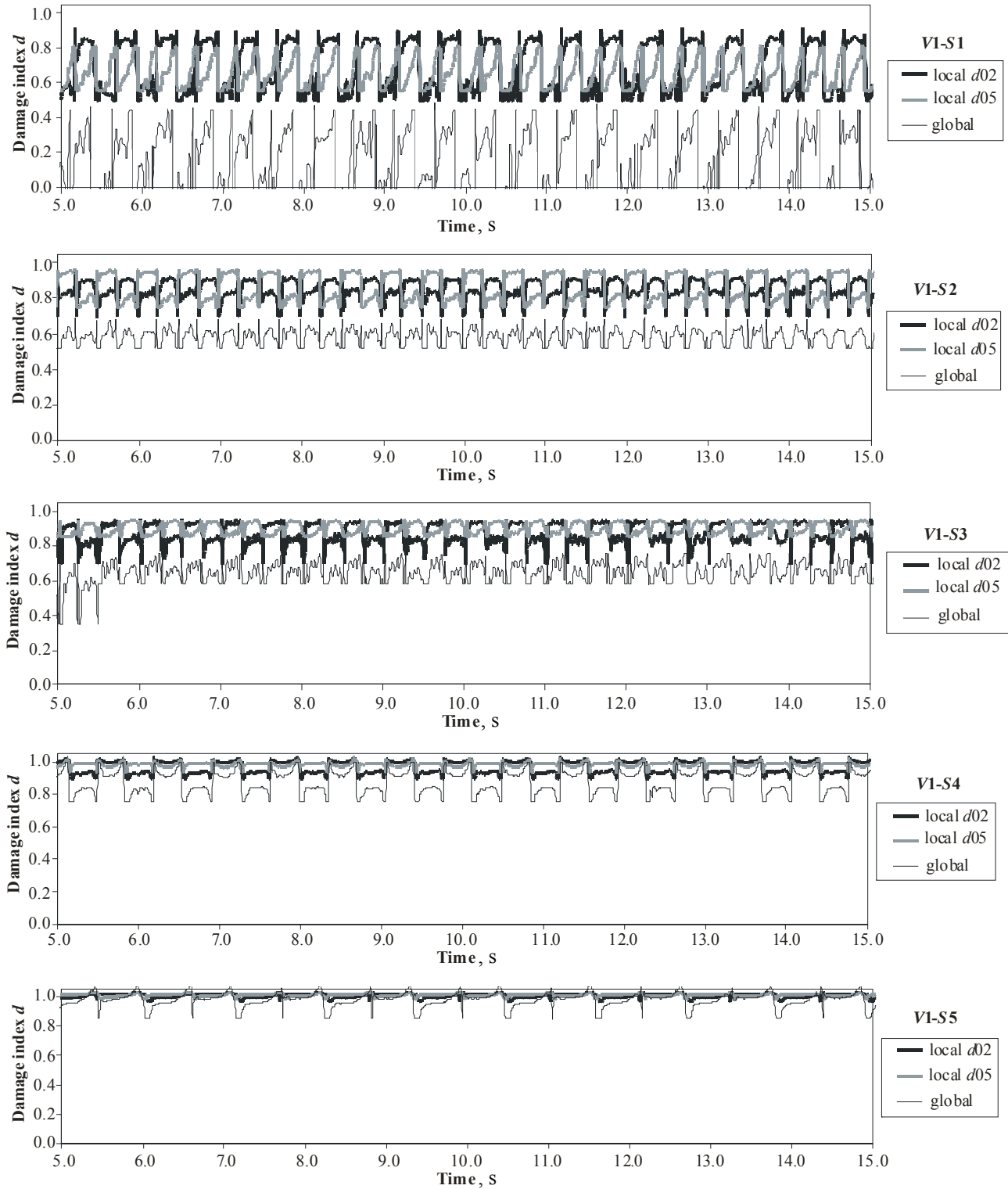
Fig. 4 Variation of the damage indices for specimen $V1$ at various loading stages
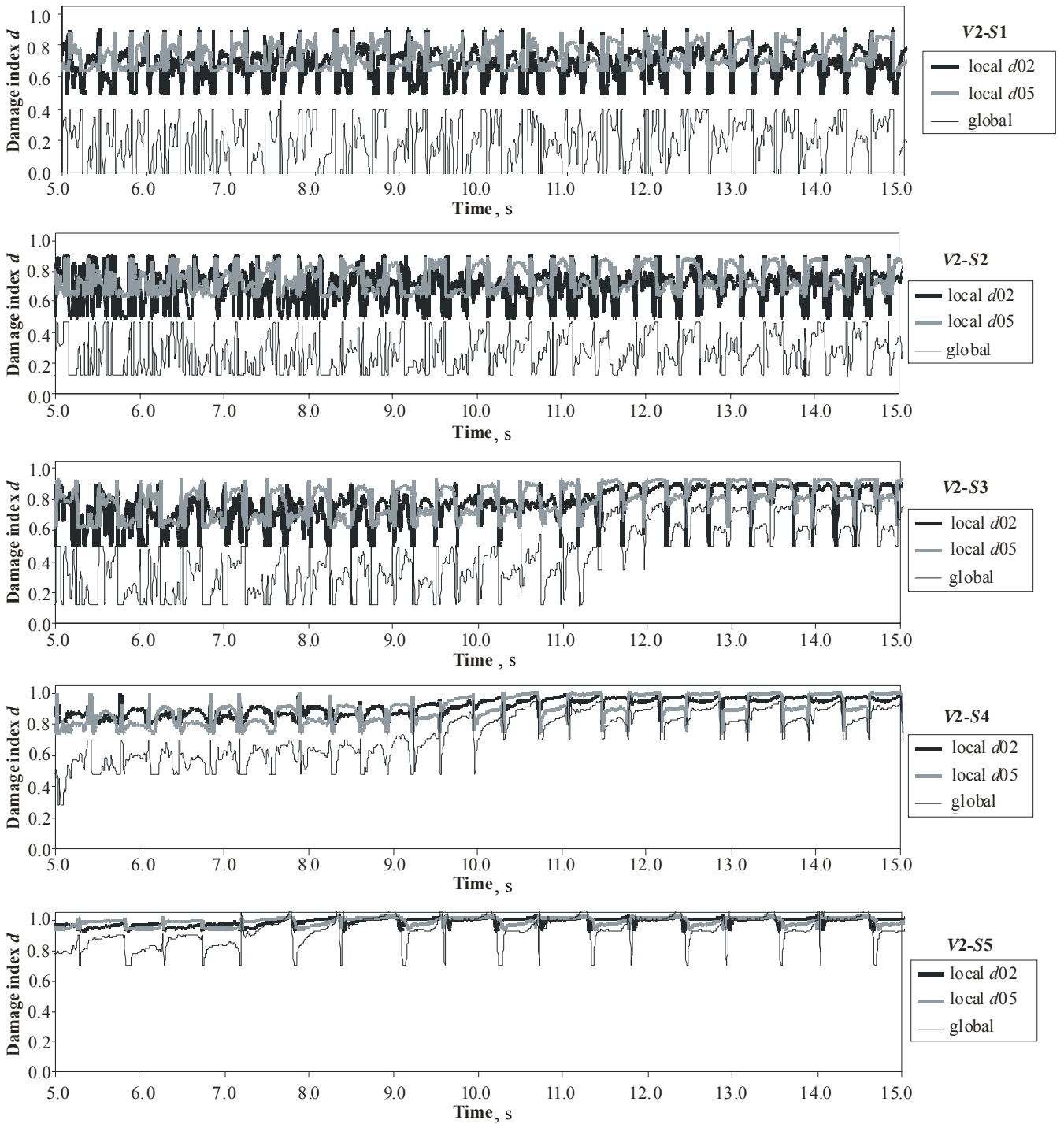
Fig. 5 Variation of the damage indices for specimen *V*2 at various loading stages

Table 1

Experimental peak values of force and displacement and corresponding stiffness and global damage index

Stage	Time interval, s	W direction				E direction			
		$|H|_{max}$, kN	$|u|$, mm	k_W, kN/mm	$d(t)$, %	H_{max}, kN	u, mm	k_E, kN/mm	$d(t)$, %
V1S1	4-4.505	7.00	3.44	2.035	0	8.62	4.38	1.969	0
	20.03-20.54	6.73	3.49	1.928	5.7	8.15	4.29	1.900	7.2
V1S2	6.06-6.6	13.68	12.27	1.114	49.3	15.61	13.69	1.140	47.9
	20.34-20.88	12.19	11.32	1.077	51.3	14.32	13.29	1.078	51.2
V1S3	5.645-6.18	19.61	19.75	0.993	55.8	15.91	18.75	0.848	63.5
	21.675-22.17	15.91	16.75	0.950	58.1	13.2	16.0	0.825	64.8
V1S4	3.29-3.99	30.25	50.67	0.597	77	19.0	27.48	0.691	71.9
	21.04-21.76	21.50	45.88	0.467	83.9	16.5	34.29	0.481	83.2
V1S5	4.465-5.655	31.85	114.9	0.277	94.1	24.05	101.7	0.236	96.3
	20.73-21.91	24.37	100.8	0.242	96.0	14.4	96.4	0.1667	100.0
V2S1	19.67-20.51	10.88	5.90	1.845	0	10.95	5.90	1.865	0
V2S2	13.13-13.63	8.40	4.56	1.842	0.2	9.96	5.35	1.862	0.2
	21.63-22.13	7.65	4.77	1.603	14.4	8.00	5.33	1.501	18.5
V2S3	11.19-11.71	15.49	15.26	1.015	49.6	13.45	10.13	1.327	31.7
	20.47-21.97	14.51	16.07	0.903	56.2	13.58	13.90	0.977	52.4
V2S4	9.95-10.71	22.80	56.40	0.404	86.0	25.45	40.60	0.627	73.0
	19.31-20.03	19.50	51.10	0.382	87.3	21.80	37.80	0.577	76.0
V2S5	10.14-11.27	17.30	95.10	0.182	99.7	18.40	59.0	0.312	91.6
	20.15-21.26	16.50	97.10	0.170	100.0	15.30	53.0	0.283	93.3

Table 2

Experimental peak values of force and strain and corresponding stiffness and local damage index

Stage	Time interval, s	W direction				E direction			
		H_{max}, kN	$e_{0,2}$, 10^5	k_W, kN	d_W, %	H_{max}, kN	$e_{0,5max}$, 10^5	k_E, kN	d_E, %
V1S1	4-4.505	7.00	47	14894	59.9	8.62	53	16264	55.9
	20.03-20.54	6.73	50	13460	64.0	8.15	62	13145	64.9
V1S2	6.06-6.6	13.68	142	9633	75.0	15.61	200	7805	80.2
	20.34-20.88	12.19	162	7525	81.0	14.32	262	5466	87.0
V1S3	5.645-6.18	19.61	201	9756	74.6	15.91	300	5303	87.4
	21.675-22.17	15.91	240	6629	83.6	13.2	320	4125	90.8
V1S4	3.29-3.99	30.25	500	6050	85.3	19.0	740	2568	95.3
	21.04-21.76	21.50	462	4654	89.3	16.5	820	2012	96.9
V1S5	4.465-5.655	31.85	1700	1874	97.3	24.05	2070	1162	99.3
	20.73-21.91	24.37	2080	1172	99.3	14.4	2300	626	100.0
V2S1	19.67-20.51	10.88	60	18133	50.5	10.95	40	27375	24.0
V2S2	13.13-13.63	8.40	80	10500	72.5	9.96	70	14229	61.7
	21.63-22.13	7.65	80	9562	75.2	8.00	80	1000	73.9
V2S3	11.19-11.71	15.49	100	15490	58.2	13.45	90	14944	89.7
	20.47-21.97	14.51	250	5804	86.0	13.58	200	6790	83.2
V2S4	9.95-10.71	22.80	500	4560	89.6	25.45	500	5090	88.0
	19.31-20.03	19.50	700	2786	94.7	21.80	730	2986	94.1
V2S5	10.14-11.27	17.30	2200	786	100.0	18.40	1000	1840	97.4
	20.15-21.26	16.50	2400	688	100.0	15.30	1360	1125	99.4

Evolution of damage in microscopic damage phase is responsible for the development of local damage.

The macrocracking phase of concrete is characterised by an increase in the number of microcracks, changes in their length and width. This phase started at the end of second stage $S2$, were horizontal force reached its value $H = 10$ kN, when due to the action of bending moment normal tensile stresses exceed compression stresses under prestressing and reached tensile resistance ($f_t = 8$ MPa). As a consequence, the first macrocrack occurred in this stage. After increasing of the load value $H = 15$ kN in the stage $S3$, normal cracks with the length of 80-140 mm developed. The relatively small 100-200 mm distances between the cracks indicate quite perfect bond between the concrete and the reinforcement. The progressively increasing macrocracking was also expanded at the stage $S4$.

Damage evolution in macroscopic damage phase indicates the development of global damage.
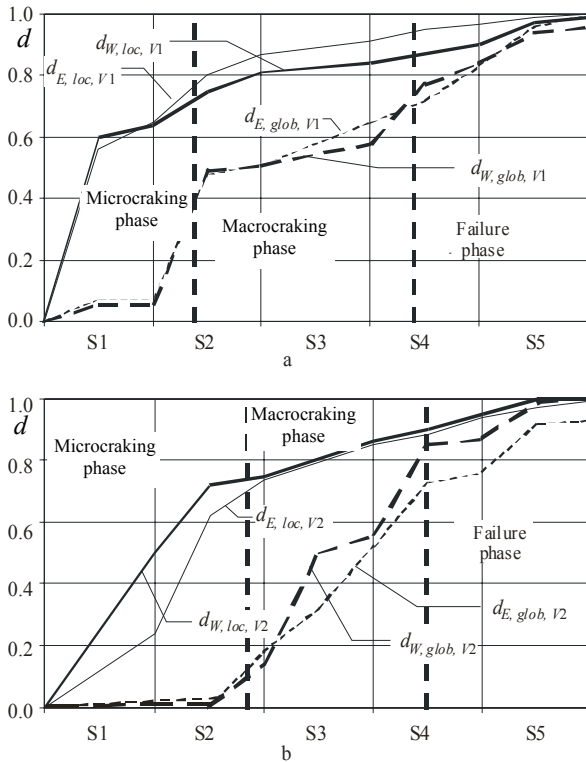
Fig. 6 Envelopes of damage indices for specimens V1 (a) and V2 (b)

The failure phase is characterised by the development of magistral through-cracks and final crashing of the column concrete at the footing. It started at in stage S5 by reaching critical value of the global damage index $d_{cr} = 0.8$. This phase indicates occurring of critical damage.

5. Conclusions

On the basis of a shaking table investigation of global and local damage of high-strength reinforced concrete columns under horizontal and vertical loading the following conclusions may be drawn.

Damage accumulation in HSC has a random character caused by the effects of different sources. Random factors provided a non-symmetric bending behaviour of an apparently symmetric specimen with an average of 10 to 15% differences in the global damage index between the opposite sides, while the difference in local damage reaches even 25%.

The comparison of global and local damage accumulation illustrates that local damage occurring at the footing accumulates significant at relatively loading level at microcracking phase. However, local damage has minor effect on the global damage, which significantly accumulates during the stages S3 and S4 during microscopic phese. Index of the global damage reached critical value $d_{cr} > 0.8$ at the end of macroscopic phase. In the final critical stage the development of both global and local damage exposes similar character.

Experimental results presented may be applied for the development of detailed damage models.

References

1. FIP/CEP, High strength concrete, State of the Art Report. SR 90/1, Bulletin d'information, No197, November 1990.-186p.
2. **Malier, Y**. L'utilisation du BHP dans une approche "système" de la construction. Les bétons à hautes performances. Caractérisation, durabilité, applications, Y. Malier (ed.), Presses Ponts et chaussées, Paris, 1992, p.3-24.
3. **Flaga, K**. Advances in materials applied in civil engineering.-J. of Material Processing Technology. 2000, 106, p.173-183.
4. **Kmita, A**. A new generation of concrete in civil engineering.-J. of Material Processing Technology. 2000, 106, p.80-86.
5. **Kudzys, A., Kliukas, R., Vadlūga, R**. Utilization of high strength spun concrete and reinforcing steel in compressive structures. Utilization of high strength concrete.-Proc.Symposium in Lillehammer, Norway, v.1, June 20-23, 1993, p.259-268.
6. **Crewe, A.J., Severn, R.T.** The European collaborative programme on evaluating the performance of shaking tables.-Philosophical Transactions of the Royal Society of London. Series A – Mathematical, Physical and Engineering sciences. 2001, 59(1786), p.1671-1696.
7. **Conte, J.P. and Trombetti, T.L.** Linear dynamic modeling of a uniaxial servo-hydraulic shaking table system.-Earthquake Engineering & Structural Dynamics. 2000, 29(9), p.1375-1404.
8. **Ogawa, N., Ohtani, K., Katayama, T., Shibata, H.** Construction of a three-dimensional, large-scale shaking table and development of core technology. - Philosophical Transactions of the Royal Society of London. Series A – Mathematical, Physical and Engineering sciences. 2001, 59 (1786), p. 1725-1751.
9. **Duarte, R.T**. Development of shaking table testing techniques.-Report of Working Group 11, 10th European Conference on Earthquake Engineering, Vienna, Austria, August/September, 1994, p. 18-65.
10. **Bairrão R., Duarte R., Vaz C., Costa A**. Portuguese methodology for the earthquake design of important structures.-Proc. of the Second Int. Conf. on Seismology and Erathquake Engineering, Teheran, Iran, May, 1995, p.114-120.
11. **Bairrão, R., Kačianauskas, R., Kliukas, R**. Experimental investigation on RC columns under horizontal and vertical loading using shaking table tests. - Civil Engineering. 1998, v.4, p.244-251.
12. **Bairrão, R., Kačianauskas, R. and Kliukas, R**. Experimental investigation of local damage in high strength concrete columns using a shaking table. - Structural Engineering and Mechanics, 2005, v.19, No5, p.581-602.

13. **Bairrão, R., Kačianauskas, R. and Kliukas, R**. Damage of high strength reinforced concrete columns under horizontal and vertical loading. -Civil Engineering and Management. 2003, 9(3), p.163-171.

14. **Bairrão, R., Kačianauskas, R. and Kliukas, R.** Local damage experimental research of high-strength concrete columns.-Proc. of fib-Symposium Concrete Structures in Seismic Regions, Athens, Greece, May, 2003, p.164-165.

15. **Качанов Л.М.** О времени разрушения при ползучести.-Изв. АН СССР, 8, 1958Б с.26-31.

16. **Lemaitre, J. and Lipman, H**. Course of damage mechanics.-New-York: Springer, 1996, p.120-143.

17. **Murakami, S. and Kamiya, K**. Constitutive and damage evolution equations of elastic-brittle materials based on irreversible thermodynamics.-Int. J. Mech. Sc. 1997, 39(4), p.473-486.

18. **Hanganu, A.D., Onate, E. and Barbat, A.H**. A finite element methodology for local/global damage evolution in civil engineering structures.-Computers&Structures, 2002, 80(20-21), p.1667-1687.

19. **Mazars, J., Ragueneau, E. and La Borderie, Ch**. Material dissipation and boundary conditions in seismic behaviour of reinforced concrete structures, in, R. de Borst (ed.), etc.-Computational modeling of concrete structures, v.1, Balkema, Roterdam, 1998, p.579-592.

R. Kliukas, R. Kačianauskas

GELŽBETONINIŲ KOLONŲ GLOBALIŲJŲ IR LOKALIŲJŲ PAŽEIDIMŲ PALYGINIMAS

R e z i u m ė

Atlikti didelio stiprumo gelžbetoninių kolonų globaliųjų ir lokaliųjų pažeidimų tyrimai. Portugalijos nacionalinėje statybos laboratorijoje naudojant vibracinį stalą buvo išbandyti du vienodi žiedinio skerspjūvio bandiniai, armuoti išilgine ir spiraline armatūra. Eksperimento metu buvo registruojami vibracinio stalo ir bandinio viršūnės horizontalieji poslinkiai, tam tikrų konstrukcijos taškų labiausiai tempiamose ir gniuždomose zonose vertikalieji poslinkiai, tiesiogiai matuojama kintanti horizontali jėga. Globaliųjų ir lokaliųjų pažeidimų atraminėse kolonų zonose palyginimas rodo, kad lokalieji pažeidimai kaupiasi daug intensyviau mikropleišėjimo stadijoje. Šie pažeidimai turi nedidelę įtaką globaliųjų pažeidimų rodikliams, kurie gerokai padidėja makropleišėjimo stadijoje. Makropleišėjimo stadijos pabaigoje globaliųjų pažeidimų indeksas pasiekia kritinę $d_{cr} > 0.8$ vertę. Paskutinėje kolonų darbo stadijoje globaliųjų ir lokaliųjų pažeidimų indeksų kreivės yra vienodo pobūdžio.

R. Kliukas, R. Kačianauskas

COMPARISON OF GLOBAL AND LOCAL DAMAGE IN REINFORCED CONCRETE COLUMNS SPECIMENS

S u m m a r y

The accumulation of global and local damage in reinforced high-strength concrete columns is experimentally investigated. Two identical column specimens with annular cross-section and spiral reinforcement were designed and two tests, up to failure, were carried out at the LNEC shaking table facility. Sine type signals, controlled in amplitude, frequency and time duration were used for these experiments. The comparison of global and local damage accumulation illustrates that local damage occurring at the footing accumulates significant of at relatively loading level at microcracking phase. However, local damage has minor effect on the global damage, which significantly accumulates during the stages *S3* and *S4* during microscopic phase. Index of the global damage reached critical value $d_{cr} > 0.8$ at the end of macroscopic phase. In the final critical stage the development of both global and local damage exposes similar character.

Р. Клюкас, Р. Качанаускас

СОПОСТАВЛЕНИЕ ЛОКАЛЬНЫХ И ГЛОБАЛЬНЫХ ПОВРЕЖДЕНИЙ В ЖЕЛЕЗОБЕТОННЫХ КОЛОННАХ

Р е з ю м е

Экспериментально исследовались глобальные и локальные повреждения высокопрочных железобетонных колонн. Два железобетонных элемента кольцевого сечения, армированные продольной и спиральной арматурой были испытаны в национальной строительной лаборатории Португалии с использованием вибрационного стола. Во время эксперимента регистрировались горизонтальные перемещения вибрационного стола и верха колонны, вертикальные перемещения определенных точек в наиболее сжатых или растянутых слоях сечений конструкций, измерялась горизонтальная циклически изменяющаяся сила. Сравнение накопления глобальных и локальных повреждений показывает, что в опорном участке колонн местные повреждения накапливаются значительно интенсивнее в стадии микрорастрескивания. Однако, местные повреждения незначительно влияют на глобальные повреждения, которые значительно вырастают в стадии макрорастрескивания. Индекс локальных повреждений достигает критической величины $d_{cr} > 0.8$ в конце стадии макрорастрескивания. В заключительной стадии накопления повреждений кривые индексов глобальных и локальных повреждений носят одинаковый характер.